Study of modulation property to incident laser by surface micro-defects on KH_2PO_4 crystal*

Chen Ming-Jun(陈明君)†, Cheng Jian(程 健), Li Ming-Quan(李明全), and Xiao Yong(肖 勇)

Center for Precision Engineering, Harbin Institute of Technology, Harbin 150001, *China*

(Received 20 October 2011; revised manuscript received 14 December 2011)

KH_2PO_4 crystal is a crucial optical component of inertial confinement fusion. Modulation of an incident laser by surface micro-defects will induce the growth of surface damage, which largely restricts the enhancement of the laser induced damage threshold. The modulation of an incident laser by using different kinds of surface defects are simulated by employing the three-dimensional finite-difference time-domain method. The results indicate that after the modulation of surface defects, the light intensity distribution inside the crystal is badly distorted, with the light intensity enhanced symmetrically. The relations between modulation properties and defect geometries (e.g., width, morphology, and depth of defects) are quite different for different defects. The modulation action is most obvious when the width of surface defects reaches 1.064 μm. For defects with smooth morphology, such as spherical pits, the degree of modulation is the smallest and the light intensity distribution seems relatively uniform. The degree of modulation increases rapidly with the increase of the depth of surface defects and becomes stable when the depth reaches a critical value. The critical depth is 1.064 μm for cuboid pits and radial cracks, while for ellipsoidal pits the value depends on both the width and the length of the defects.

Keywords: KH_2PO_4 crystal, surface defects, modulation degree, three-dimensional finite-difference time-domain

PACS: 42.60.Jf, 77.84.Fa, 46.15.–x, 42.62.–b **DOI:** 10.1088/1674-1056/21/6/064212

1. Introduction

KH_2PO_4 (potassium dihydrogen phosphate, KDP for short) crystals are widely used in inertial confinement fusion (ICF) as terminal frequency converters and optical switch–Pockels cells.[1,2] The laser induced damage threshold (LIDT), which is a vital index for KDP crystal, has restricted the application and development of the ICF program for last five decades.[3] However, resistance against laser induced damage in order to enhance LIDT still remains a technological challenge. Currently, researchers' work on LIDT focuses on intrinsic aspects such as thermal effect, multiphoton ionization, impact ionization, impurity content, multi-wavelength, and so on, while studies on the superficial aspects in KDP crystal are insufficient.[4–6]

KDP crystals are considered to be one of the most difficult optical materials to fabricate because they require a long fabrication time, and they are extremely soft, fragile, deliquescent, easy to craze, and sensitive to temperature variation.[7] In addition, under the illumination of a high-peak-power laser beam, some laser-induced damage spots would be found on the surface of KDP crystal during the fracture process, and sequentially become surface micro-defects. These surface micro-defects are mainly present in three forms: superficial burns, micro-cracks, and micro-pits, with characteristic dimensions ranging from micrometer to sub-millimeter. However, an incident laser could potentially be modulated by using surface defects, leading to a non-uniform distribution of light intensity and local energy concentration, and a nonlinear increase of the intense laser.[4] As a result, the laser induced damage threshold declines.

So far, there have been some reports about the modulation properties of surface defects in the optical components of an incident laser. Crisp *et al.*[8] studied the important influence of Fresnel reflections on the surface damage threshold of ideal transparent dielectric materials (without any defects). Bonneau *et al.*[9] carried out two-dimensional (2D) simulation of electrical field distribution in the vicinity of planar cracks by using the finite element code PALAS. Genin *et al.*[10] numerically calculated the light intensity distribution of an initially plane wave incident on planar and conical surface cracks by using the TEMPEST code and discussed the role of light intensity enhancement in optical breakdown. Chen *et al.*[11] analysed the effect of

*Project supported by the National Natural Science Foundation of China (Grant No. 50875066).

†Corresponding author. E-mail: chenmj@hit.edu.cn

© 2012 Chinese Physical Society and IOP Publishing Ltd

superficial micro-waviness on the LIDT of KDP crystal with the Fourier model method, which is mainly used to perform 2D simulations of periodic structures. However, most of these studies have just focused on fused silica, or simulated the surface defects with periodic structures like superficial micro-waviness.

In this paper, we simplify the surface defects into three ideal forms: cuboid pits, radial cracks, and ellipsoidal pits. Numerical simulation of incident laser modulation by using these three kinds of surface defects is performed by employing the three-dimensional (3D) finite-difference time-domain (3D FDTD) method, which was developed to solve the Maxwell equation. The relationships between modulation degree and the structural parameters of different surface defects are given in detail. This work can not only provide a theoretical basis for the laser induced damage mechanism, but also contributes to the preliminary preparation work for repairing laser induced damage in KDP crystals.

2. Model and theory

In the practical applications of KDP crystal, the morphology of surface defects created during both fabrication and exposure to the laser is considerably complex.[12,13] Figure 1(a) shows images of actual bulk damage sites in KDP crystal irradiated by a 355-nm laser. As can be seen from the morphology in Fig. 1(a), the damage sites are a mixture of melting pits and cracks. According to their morphology, we simplify the surface defects into three ideal forms, as demonstrated in Fig. 1(b).

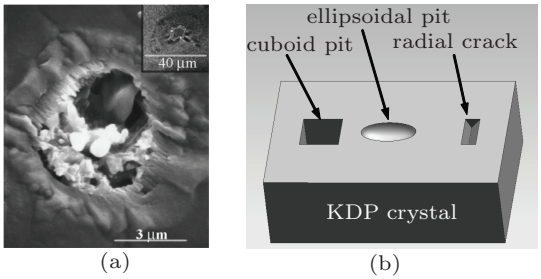


Fig. 1. Images of KDP damage sites and the model of surface defects for numerical simulations: (a) morphology of actual damage sites initiated with 3ω light;[13] (b) 3D schematic diagram of the three simplified kinds of surface defects in this paper.

Light is a special kind of electromagnetic wave, so the process of laser irradiation can be considered as the propagation of an electromagnetic wave through KDP crystal, which satisfies the Maxwell equation. Based on the rigorous electromagnetic field theory, the 3D FDTD method is used to solve the Maxwell equation to obtain the electric field intensity distribution.[14,15] For KDP crystal, the relative dielectric constant $\varepsilon_{\rm r}$ is 1.49^2 (n_1^2), and two other electromagnetic parameters (relative magnetic permeability $\mu_{\rm r}$ and electric conductivity σ) are 1.0 and 0, respectively. Figures 2–4 show the 3D FDTD models of a surface cuboid pit, a radial crack, and an ellipsoidal pit for numerical calculations, respectively. Figures 2(b), 3(b), and 4(b) show the xoz sections at $y = 0$ μm, and Figs. 2(c), 3(c), and 4(c) exhibit the yoz sections at $x = 0$ μm.

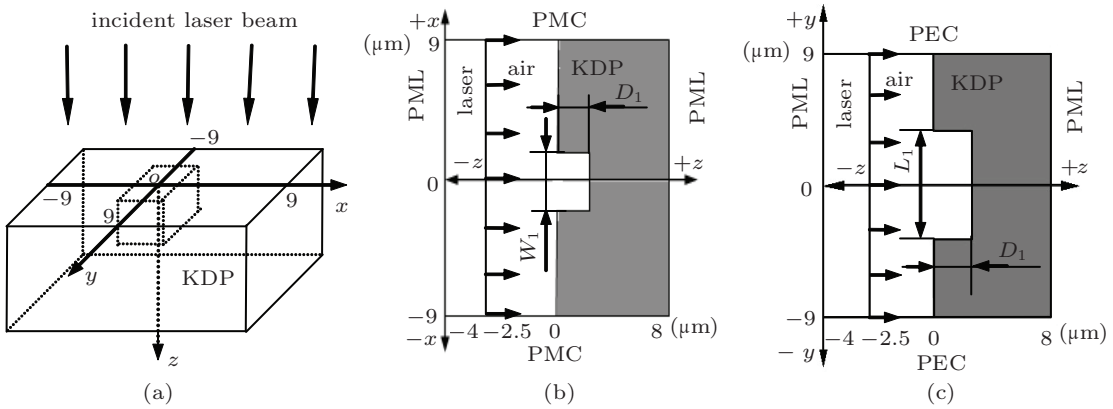


Fig. 2. 3D FDTD model of a cuboid pit, showing: (a) the space model of a cuboid pit; (b) the xoz section at $y = 0$ μm; and (c) the yoz section at $x = 0$ μm.

As shown in Figs. 2–4, all the surface defects are assumed to be on the input surface and all the defects are further assumed to be empty (relative dielectric constant $\varepsilon_0 = 1.0$). During numerical simulation, a 1ω ($\lambda = 1.064$ μm) laser with an electric field intensity normalized to 1 V/m irradiates in the direction normal to the front surface of the KDP crystal, namely along the $+z$ axis. A time-harmonic plane

wave is adopted in this work. The different grid size is $\delta = 0.05$ μm, which is less than $\lambda/12$ in order to reduce numerical dispersion caused by the difference in the 3D FDTD.[15] The whole calculated domain is −9 μm–+9 μm in the x direction, −9 μm–+9 μm in the y direction, and −4 μm–+8 μm in the z direction, respectively. To avoid the reflection of light at the boundary truncation, the perfectly matched layer (PML) boundary condition is adopted in the x–y transverse planes ($\pm z$ edges).[16,17] Moreover, the input wave is assumed to be in the y-direction polarization (TE mode), so the perfect electrical conductor (PEC) is set to be in the x–z transverse planes ($\pm y$ edges) and the perfect magnetic conductor (PMC) is set to be in the y–z transverse planes ($\pm x$ edges) to realize the plane wave[18] (as seen in Figs. 2–4).

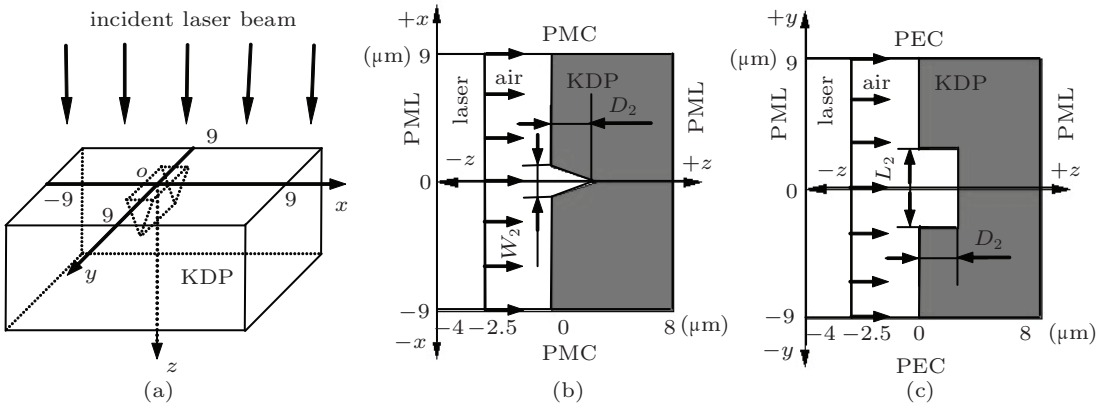


Fig. 3. 3D FDTD model of a radial crack, showing: (a) the space model of the radial crack; (b) the xoz section at $y = 0$ μm; and (c) the yoz section at $x = 0$ μm.

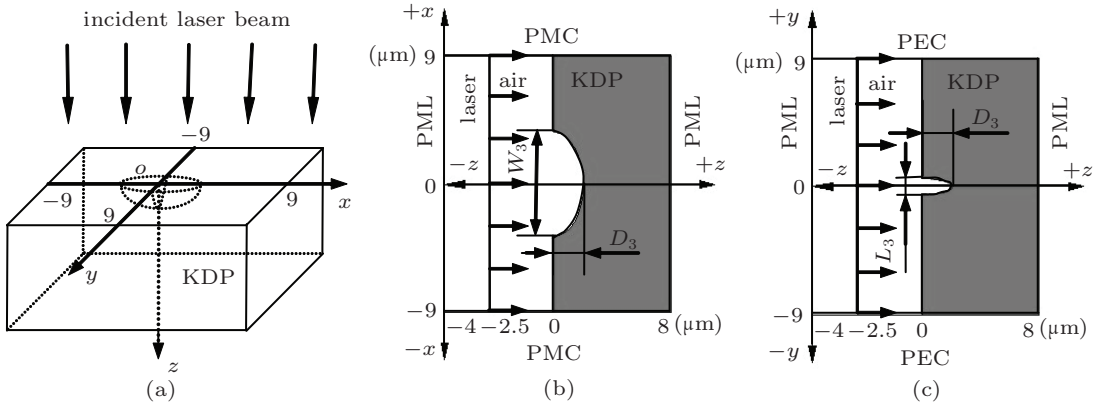


Fig. 4. 3D FDTD model of an ellipsoidal pit, showing: (a) the space model of an ellipsoidal pit; (b) the xoz section at $y = 0$ μm; and (c) the yoz section at $x = 0$ μm.

Light intensity is introduced to describe the distribution of energy inside the KDP crystal. It is the average of the electromagnetic field energy-flux density within a period of the input wave, and can be calculated using the following equation:[19]

$$I = \frac{1}{2}\left|\mathrm{Re}(\boldsymbol{E} \times \boldsymbol{H}^*)\right|. \tag{1}$$

The light intensity distribution inside the crystal must be fully considered during the laser irradiation in ICF. If the peak light intensity exceeds the critical value in a certain region, it will lead to some unwanted effects such as multi-photon ionization, electrical avalanche breakdown, heat absorption, etc.

To quantitatively describe the incident laser modulation effects by using surface defects, the light intensity modulation degree is defined as follows:

$$M_{\mathrm{I}} = I_{\max}/I_0, \tag{2}$$

where I_0 is the light intensity (inside the crystal) under ideal conditions (without any defects), and $I_{\max}$ is the maximum light intensity after the surface defect modulation. From the viewpoint of resistance against failure, we can evaluate the system security by means of the degree of modulation. That is to say, the bigger the degree of modulation, the more easily the optical component will be broken down.[20]

3. Result and discussion

As shown in Figs. 2, 3, and 4, there are three structural parameters in x, y, and z directions for these three kinds of defects. The parameters are symbolized by W_i, L_i, and D_i (where $i = 1, 2, 3$ and stand for cuboid pit, radial crack, and ellipsoidal pit, respectively). At first, the light intensity distribution inside the KDP crystal under ideal conditions is calculated. It is found that the light intensity distributes uniformly and the light intensity $I_0 = 1.2973 \times 10^{-3}$ W/m^2. For a TM mode wave with normal incidence, the transmission coefficient can be obtained as $r = E_t/E_i = 2 \cdot n_0/(n_0 + n_1) = 0.8032$ according to the law of Fresnel reflections.[8] The incident wave is normalized to 1 V/m, so the electric field inside the crystal is $E_t = 0.8032$ V/m. Sequentially, the corresponding light intensity is calculated from Eq. (1) as

$$I = \frac{1}{2}\left|\mathrm{Re}(\boldsymbol{E} \times \boldsymbol{H}^*)\right| = \frac{1}{2}\sqrt{\frac{\varepsilon_1}{\mu_1}}\left|E_t\right|^2 = 1.2756 \times 10^{-3}\ \mathrm{W/m^2}.$$

The theoretically derived light intensity value is well consistent with the numerically simulated results with an error of less than 2%. Such agreement validates the 3D FDTD model and simulation conditions that have been selected in this study.

3.1. Incident laser modulation by using surface defects

The light intensity distributions after the modulation of these three kinds of surface defects are similar under the same structural parameters and exposure conditions, so we take a radial crack as an example to reveal the modulation law of surface defects. Since the uniform plane wave is adopted as an input wave and the defect centre is located at the origin of coordinates, it is easy to find that the light intensity distribution is symmetrical about the xoz cross section. The light intensity distributions in x–z planes for given y values (y = 0 μm, 0.4 μm, 1 μm, 2 μm, 8 μm) are shown in Fig. 5. The parameters are $L_2 = \lambda$, $W_2 = \lambda$, and $D_2 = \lambda$. From Fig. 5, we can see that the light intensity distribution inside the KDP crystal is modulated to different modulation degrees, and the modulation action is more notable in the x–z cross sections with smaller y-value. In Figs. 5(b)–5(f), the modulation degrees are 2.0864, 1.8826, 1.5318, 1.3442, and 1.1100, respectively. The modulating action is the most obvious in the central plane (y = 0 μm). So in this paper, we focus on the light intensity distribution in this cross section.

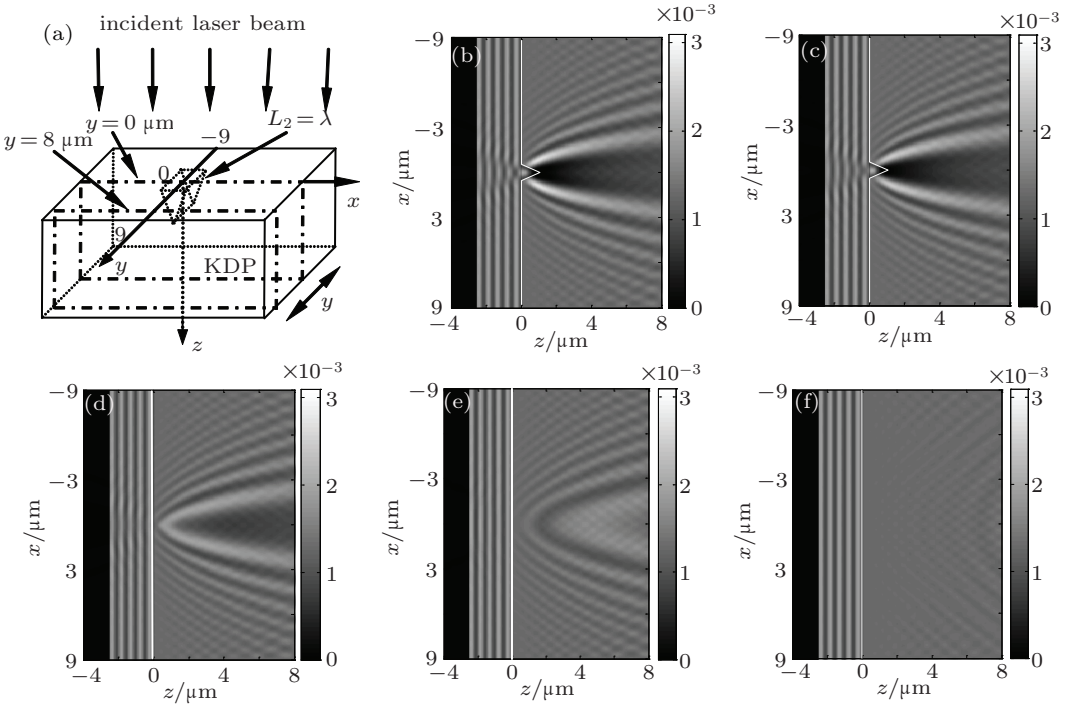


Fig. 5. Light intensity distribution after the modulation of an input surface crack with $L_2 = W_2 = D_2 = \lambda$ in x–z planes for given y values. (a) Schematic diagram of a radial crack and x–z cross planes at $y = 0$ (b), 0.4 (c), 1 (d), 2 (e), 8 μm (f). (The white line indicates the interface between air and crystal, the area on the right is inside the crystal; there is no crack in the cases of (d), (e), and (f), because the crack length is 1.064 μm.)

The light intensity profile in Fig. 5(b) clearly demonstrates that the ideal light is evidently distorted by the modulation of the surface crack. Light intensity enhancement emerges inside the crystal and is symmetrically distributed. The explanation for this phenomenon is that the transmitting wave through the surface crack overlaps with the incident wave inside the crystal, and they satisfy the conditions of constructive interference.[4,21] According to the simulation results in Fig. 5(b), the maximal light intensity is 2.7067×10^{-3} W/m^2 and the modulation degree $M_{\rm I}$ is 2.0864, at $x = \pm0.8$ μm, $y = 0$ μm, and $z = 0.9$ μm. The local light intensity peak implies an energy concentration which may cause some unwanted effects such as electric avalanche breakdown, heat absorption, and so on. For this reason, the dependence of local energy concentration on the modulation properties of surface defects must be profoundly investigated to avoid surface damage growth of the KDP crystal.

3.2. Modulation property of the width of the surface defect

The light intensity distribution profiles are similar for all three kinds of surface defects, but the modulation degrees differ largely from each other. So it is very important to discuss the role of the structural parameters of different defects in modulating the light intensity. Figure 6 shows the curves of modulation degrees with respect to the width for the three kinds of surface defects.

In Fig. 6, it is demonstrated that the variations of modulation degree with width for different defects are obviously different. For $W_i < 1\lambda$, the tendency of each curve is similar, and especially for radial cracks and ellipsoidal pits, they almost overlap. The curves ascend sharply and reach peak values simultaneously when W_i is about 1λ. The peak values are 2.3663, 2.0836, and 2.0234, respectively. For $W_i > 1\lambda$, the curve for cuboid pits first slightly decreases and then becomes nearly unchanged at 2.1800. However, the other two curves for radial cracks and ellipsoidal pits droop gradually, and then later decreases more rapidly. The phenomena illustrate that the effects of defect width on modulation property differ from each other. Cuboid pits modulate the incident wave most violently, while the modulation effect of ellipsoidal pits is relatively small. This is reasonable, since the morphology of defects such as ellipsoidal pits is more regular than those of cuboid pits and radial cracks, which would cause more complex light interference inside the crystal. Therefore, we should pay attention to cuboid pits and radial cracks, especially when W_i is around 1λ or greater than 1λ for cuboid pits in the actual mechanical process of KDP crystal.

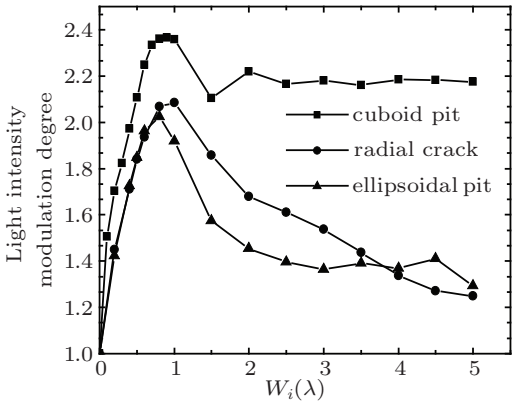


Fig. 6. Modulation property curves with respect to width for three different surface defects. During the variation of width, the other two parameters L_i and D_i keep constant ($L_i = D_i = \lambda$).

3.3. Modulation property of the surface defect morphology

Table 1 shows the light intensity modulation degrees of different surface defects with given depths. Since spherical pits can be obtained easily by micromachining in the practical repair process of laser induced damage spots, we focus on the modulation property of surface defects with spherical morphology instead of ellipsoidal morphology. From Table 1, it can be seen that after the modulation of surface defects, the light intensity enhancement for cuboid pits and radial cracks is greater than that for spherical pits for the given defect depths. The modulation degrees all become larger with the increase of defect depth, but the modulation degree grows the slowest for spherical pits.

Table 1. Modulation degrees of surface defects with various geometries.

Defect length	Defect width	Defect depth	Light intensity modulation degree		
$L_i(\lambda)$	$W_i(\lambda)$	$D_i(\lambda)$	Cuboid pits	Radial cracks	Spherical pits
2	2	0.2	1.6520	1.3470	1.2108
2	2	0.4	2.2341	1.6951	1.4282
2	2	0.5	2.4102	1.8442	1.5318
2	2	0.6	2.4808	2.0055	1.6330
2	2	0.8	2.4715	2.3112	1.7748
2	2	1.0	2.7123	2.6176	1.8466

For a given depth $D_i = 0.6\lambda$, the light intensity distributions of cuboid pits, radial cracks, and spherical pits are shown in Fig. 7. It is shown in Fig. 7 that the modulation of surface defects makes the light field greatly distorted, thereby resulting in discontinuous bands with an enhanced light intensity. There are two main bands under both sides of the defects along the light travelling direction. For the light intensity distribution in Fig. 7(a), there is a more light intensty enhanced band just under the cuboid pits, and a peak light intensity of 3.2×10^{-3} W/m^2 ($M_i = 2.4808$) is reached in this region at $x = 0$ μm, $z = 1.75$ μm. However, the values of peak light intensity for radial cracks and spherical pits (shown in Figs. 7(b) and 7(c)) are inside the defects (outside the crystal) and the modulation degrees are 2.0055 and 1.6330, respectively. Moreover, from Fig. 7(c), we can see that the modulating action is the smallest for spherical pits and the light intensity distribution is relatively uniform. This is because the morphologies of different surface defects will cause various path-length differences between incident and transmitting beams and result in the weak interference of smooth morphologies like spherical pits and the constructive interference for defects like cuboid pits and radial cracks.[10] Therefore, in the actual use of KDP crystal we could repair the initial laser induced damage spots into smooth morphologies such as spherical and Gaussian shaped contours by micromachining. In this way, we can enhance the induced damage resistance of KDP crystal.

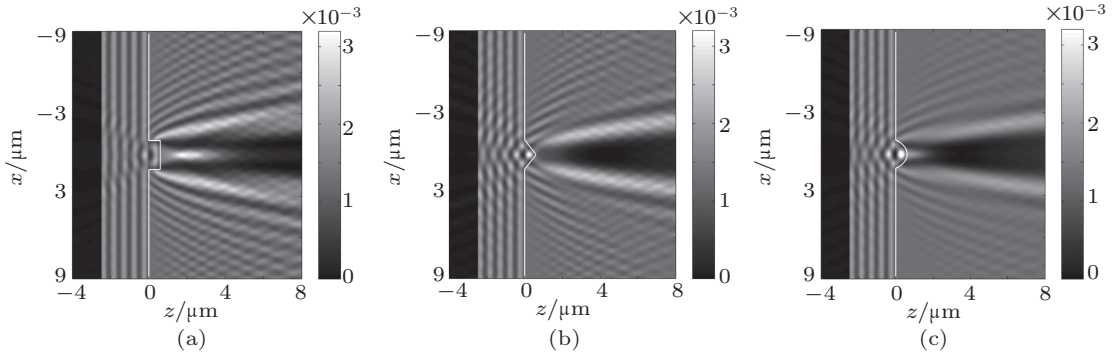


Fig. 7. Light intensity distributions after the modulations of different kinds of surface defects with $L_i = W_i = \lambda$, $D_i = 0.6\lambda$: (a) cuboid pits; (b) radial cracks; and (c) spherical pits. (The white line indicates the interface between air and crystal, the area on the right is inside the crystal.)

In early studies, the mitigation of laser-initiated surface damage sites was successfully achieved by micro-machining using carbide and diamond cutting tools.[22] Spherical and elongated, banana-shaped morphologies were machined on KDP crystal surfaces and they proved to be stable after subsequent hundreds of shots at 351 nm, fluences ranging from 2 J/cm^2 to 13 J/cm^2, and about 11-ns pulse length.[22] According to these previous experimental studies, our simulation results indirectly confirm that surface defects with smooth morphology are conducive to light propagation and laser induced damage. Thus the mechanism of enhanced damage resistance by micromachining for KDP crystal may be better understood from the viewpoint of modulation by using surface defects with different morphologies.

3.4. Modulation property of the depth of the surface defect

The modulation property curves with respect to the depth of cuboid pits and radial cracks are given in Figs. 8 and 9. In Fig. 8, it can be found that the four curves for given widths share a similar trend. For each curve, it first ascends rapidly until $D_1 = 1\lambda$, then becomes nearly stable when $D_1 > 1\lambda$. The maximal modulation degrees are 2.1230, 2.3437, 2.1880, and 2.1377, respectively. The above phenomena demonstrate that for different given widths the modulation action seems to be significant when the depth is more than 1λ, especially when the width is 1λ , which is consistent with the result of Fig. 6. By comparing Fig. 8 with Fig. 9, we find that the curvilinear trend in Fig. 9 is similar to that in Fig. 8 and the modulation action is also greatest at $W_i = 1\lambda$. However, there are some differences between them. For example, for $D_i < 1\lambda$, the ascending speed in Fig. 8 is slower than in Fig. 9 and

when the depth is above 1λ, the stable modulation degrees for radial cracks are 1.9760, 2.2516, 1.9291, and 1.8271, which are all smaller than those in the case of cuboid pits. From the above discussion, we can conclude that for cuboid pits and radial cracks, when $D_i < 1\lambda$, the modulation property curves rise with the increase of depth and they rise faster for cuboid pits; when $D_i > 1\lambda$, the modulation degree becomes stable and is determined only by the width of the defect.

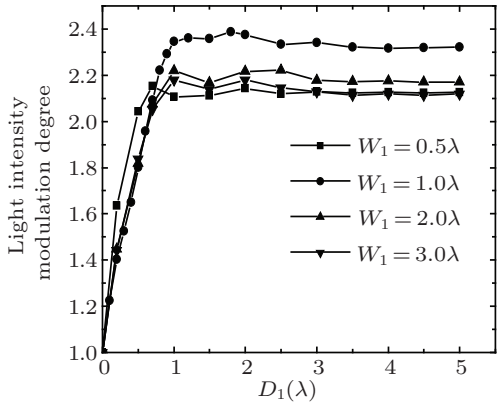


Fig. 8. Modulation property curves with respect to the depth of cuboid pits for given widths: 0.5λ, 1.0λ, 2.0λ, and 3.0λ, with length L_1 keeping constant ($L_1 = \lambda$) during the increase of depth.

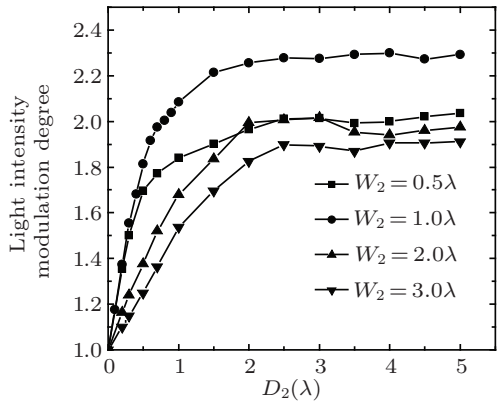


Fig. 9. Modulation property curves with respect to the depth of radial cracks for given widths: 0.5λ, 1.0λ, 2.0λ, and 3.0λ, with length L_2 keeping constant ($L_2 = \lambda$) during the increase of depth.

Figure 10 shows the variations of the degree of light intensity modulation with the increase of depth of ellipsoidal pits for different pit widths. From Fig. 10, it can be seen that the curves ascend sharply at the beginning and then become constant when D_3 reaches a critical value. The stable modulation degrees for the three curves are 1.5802, 2.0084, and 2.2391, respectively, which are positively correlated with both the length dimension and the width dimension. Furthermore, the critical depths for the three curves are about 0.5λ, 1.0λ, and 2.0λ, respectively, which are equal to both the length and the width of the defects correspondingly. Therefore, in the actual repair process of KDP crystal, we can determine the machining depth by the size of the damage area through referring to the theoretical simulation results.

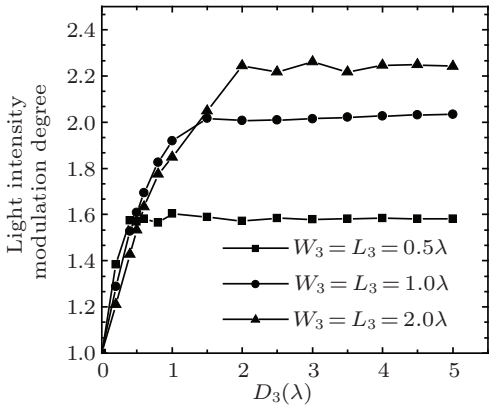


Fig. 10. Modulation property curves with respect to the depth of ellipsoidal pits for given widths and lengths. The lengths L_3 and widths W_3 are both equal to 0.5λ, 1.0λ, and 2.0λ, respectively.

4. Conclusion

The modulation properties of three simplified forms of surface defects inside KDP crystal are quantitatively investigated by numerical simulation using the 3D finite-difference time-domain method. The conclusions drawn from the study are as follows.

(i) The light intensity distribution in the *xoz* cross section ($y = 0$ μm) is distorted most obviously after the modulation by surface defects. The local enhancement of light intensity is present in this plane and distributed symmetrically.

(ii) With the variation of defect width, cuboid pits modulate the incident wave most seriously, while the ellipsoidal pit modulation is relatively weak. For the three types of defects, the modulation degrees all reach their peak values when W_i equals λ.

(iii) The defect morphology plays a significant role in the modulation action of surface defects. For spherical pits, the light intensity distribution seems more uniform and the modulation degree is much smaller than those of cuboid pits and radial cracks.

(iv) The modulation degree ascends rapidly with the increase of defect depth, and becomes stable when the depth reaches a critical value. The critical depth for cuboid pits and radial cracks is λ, while for ellipsoidal pits, it depends on both the width and the length of the defect.

References

[1] Negress R A, Kucheyev S O, DeMange P, Bostedt C, Buuren T V, Nelson A J and Demos S G 2005 *Appl. Phys. Lett.* **86** 171107

[2] DeYoreo J J, Burnham A K and Whitman P K 2002 *Int. Mater. Rev.* **47** 113

[3] Carr A W, Radousky H B, Rubenchik A M, Feit M D and Demos S G 2004 *Phys. Rev. Lett.* **92** 087401

[4] Bloembergen N 1973 *Appl. Opt.* **12** 661

[5] Manenkov A A 2008. *Proc. SPIE* **7132** 713202

[6] Reyné S, Duchateau G, Natoli J Y and Lamaignère L 2011 *Proc. SPIE* **7937** 79370L

[7] Xu Q, Wang J, Li W, Zeng X and Jing S Y 1999 *Proc. SPIE* **3862** 236

[8] Crisp M D, Boling N L and Dubé G 1972 *Appl. Phys. Lett.* **21** 364

[9] Bonneam F, Combis P, Pujols A, Rullier J L, Sesques M and Vierne J 2003 *Proc. SPIE* **4932** 250

[10] Génin F Y, Salleo A, Pistor T V and Chase L L 2001 *J. Opt. Soc. Am.* A **18** 2607

[11] Chen M J, Li M Q, Jiang W and Xu Q 2010 *J. Appl. Phys.* **108** 043109

[12] DeMange P, Carr C W, Radousky H B and Demos S G 2004 *Rev. Sci. Instrum.* **75** 3298

[13] Carr C W, Feit M D, Johnson M A and Rubenchik A M 2006 *Appl. Phys. Lett.* **89** 131901

[14] Sullivan D M 2000 *Electromagnetic Simulation Using the FDTD Method* (New York: IEEE Press) pp. 79–89

[15] Ge D B and Yan Y B 2002 *Finite-Difference Time-Domain Method for Electromagnetic Waves* (Xi'an: Xidian University Press) pp. 10–28 (in Chinese)

[16] Gedney S D 1996 *IEEE T. Antenn. Propag.* **44** 1630

[17] Fujii M, Omaki N, Tahara M, Sakagami I, Poulton C, Freude W and Russer P 2005 *IEEE J. Quantum Elect.* **41** 448

[18] Cao Q S and Chen Y C 2003 *IEEE T. Antenn. Propag.* **51** 350

[19] Zhou K D, Zhang X W, Dong T L and Gu C L 2000 *Electromagnetic Field Theory Fundamentals* (Beijing: China Machine Press) pp. 247–248 (in Chinese)

[20] Chen M J, Jiang W, Li M Q and Chen K N 2010 *Chin. Phys.* B **19** 064203

[21] Li L, Xiang X, Zu X T, Wang H J, Yuan X D, Jiang X D, Zheng W G and Dai W 2011 *Chin. Phys.* B **20** 074209

[22] Hrubesh L W, Brusasco R B, Grundler W, Norton M A, Donohue E E, Molander W A, Thompson S L, Strodtbeck S R, Whitman P K, Shirk M D, Wegner P J, Nostrand M C and Burnham A K 2003 *Proc. SPIE* **4932** 180